English Summary:

Stabilization of unstable fixed point

Stab. boundaries : $\mathrm{Re}\,\Lambda = 0$ $\Rightarrow$

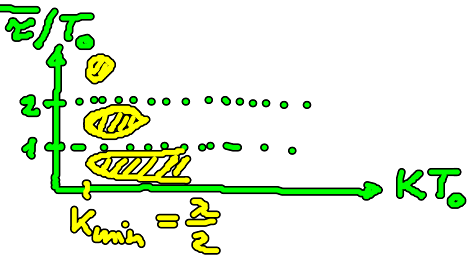

multiple feedback (ETDAS):

$$K \sum_{n=0}^{\infty} R^n \left[x(t-n\tau) - x(t-(n+1)\tau) \right]$$

$(0 \leq R < 1)$

$$\Rightarrow \boxed{\Lambda + K \frac{1-e^{-\Lambda\tau}}{1-Re^{-\Lambda\tau}} = \lambda + i\omega}$$

Stabilisierung instab. period. Orbits:

subkrit. Hopf-Bif.: $\boxed{\dot{z} = (\lambda + i\omega + (1+i\gamma)|z|^2)z + b(z(t-\tau)-z(t))}$

$\lambda < 0, \ \omega = 1, \ \gamma < 0, \quad b = b_0 e^{i\beta} \in \mathbb{C}$

nichtinvasive Kontrolle:

Wähle $\tau \overset{!}{=} nT = \dfrac{2\pi n}{1-\gamma\lambda}$ $\quad$ (T = Periode des UPO)

(Pyragas-Kurve in der (τ,λ)-Ebene)

Hopf-Kurve: lin. Stab. des Fixp. $z(t) \sim e^{\eta t}$

$$\eta + b(1-e^{-\eta\tau}) = \lambda + i \qquad \text{vgl. } 3.2.1$$

Hopf-Bif.: $\eta = i\omega$: $\quad 0 = \lambda + b_0\left[\cos(\beta-\omega\tau) - \cos\beta\right]$ $\quad$ (1)

$\omega - 1 = b_0\left[\sin(\beta-\omega\tau) - \sin\beta\right]$ $\quad$ (2)

(1) $\Rightarrow \omega\tau = \pm \arccos\left(\dfrac{b_0\cos\beta - \lambda}{b_0}\right) + \beta + 2\pi n$

$$\left.\begin{aligned} \left(\frac{b_0\cos\beta-\lambda}{b_0}\right)^2 &= \cos^2(\beta-\omega\tau) \\ \left(\frac{\omega-1+b_0\sin\beta}{b_0}\right)^2 &= \sin^2(\beta-\omega\tau) \end{aligned}\right\} \cos^2 + \sin^2 = 1 \qquad (3)$$

$\overset{(3)}{\Rightarrow} \omega = g(\lambda, b_0, \beta) \overset{\text{elim.}}{\Longrightarrow} \tau = h(\lambda, b_0, \beta)$

Hopf-Kurven in (τ, λ)-Ebene

ohne Kontrolle $(b=0)$: subkrit. Hopf

mit Kontrolle $b = b_0 e^{i\beta}$ superkrit. Hopf entlang der Pyragaskurve

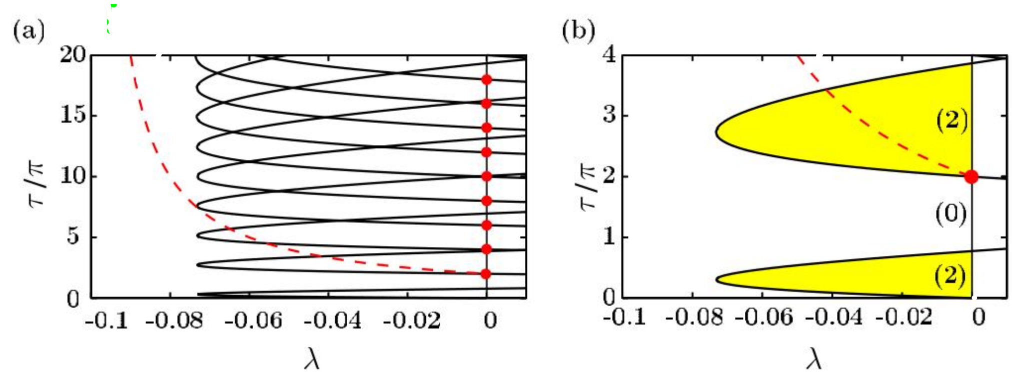

Fiedler et al. PRL 98, 114101 (2007)

FIG. 1 (color online). Pyragas (red dashed) and Hopf (black solid) curves in the (λ, τ) plane: (a) Hopf bifurcation curves $n = 0, \ldots, 10$, (b) Hopf bifurcation curves $n = 0, 1$ in an enlarged scale. Yellow (light gray) shading marks the domains of unstable $z = 0$ and numbers in parentheses denote the dimension of the unstable manifold of $z = 0$ ($\gamma = -10$, $b_0 = 0.3$, and $\beta = \pi/4$).

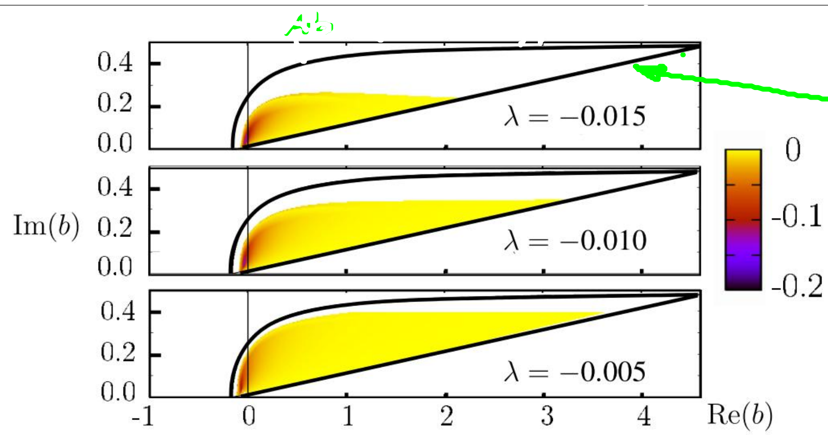

analyt. Bed.

$\tau_{Hopf}(\lambda) < \tau^{(2)}_{Pyragas}$

Koppl.phase $\beta \neq 0$!

FIG. 3 (color online). Domain of control in the plane of the complex feedback gain $b = b_0 e^{i\beta}$ for three different values of the bifurcation parameter λ. The black solid curves indicate the boundary of stability in the limit $\lambda \nearrow 0$; see (18) and (19). The color-shading shows the magnitude of the largest (negative) real part of the Floquet exponents of the periodic orbit ($\gamma = -10$, $\tau = \frac{2\pi}{1-\gamma\lambda}$).

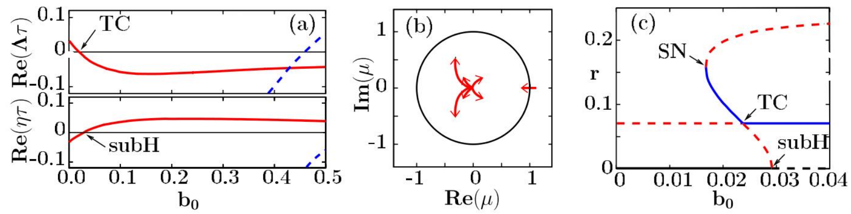

FIG. 2 (color online). (a) Top: Real part of Floquet exponents Λ of the periodic orbit vs feedback amplitude b_0. Bottom: Real part of eigenvalue η of the steady state vs feedback amplitude b_0. (b) Floquet multipliers $\mu = \exp(\Lambda\tau)$ in the complex plane with the feedback amplitude $b_0 \in [0, 0.3]$ as a parameter. (c) Radii of periodic orbits. Solid (dashed) lines correspond to stable (unstable) orbits. ($\lambda = -0.005$, $\gamma = -10$, $\tau = \frac{2\pi}{1-\gamma\lambda}$, $\beta = \pi/4$).

korrektes Odd-Number-Theorem: E.W. Hooton, A. Amann, PRL 109, 154101 (2012)

Analytical Limitation for time-delayed feedback control in Autonomous Systems

A. Amann, E.W. Hooton: Phil. Trans. R. Soc. A (2013)

exp. Verifikation durch Laserexperiment (Schikora, Wünsche, Henneberger 2011)

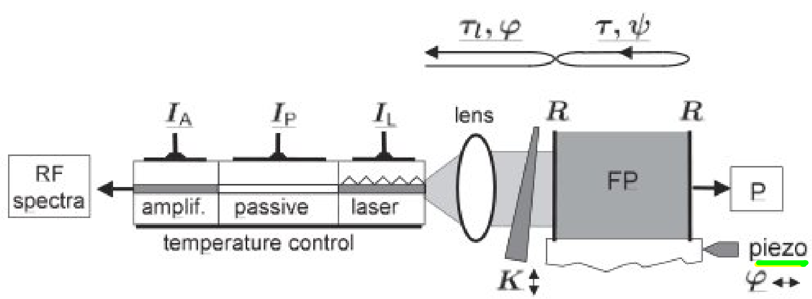

FIG. 1. All-optical control setup: multisection laser with optical feedback from a planar FP glass etalon. rf spectra: 50-GHz photo diode and electrical spectrum analyzer. P: power measurement by infrared photodiode. R: reflectivity of the FP mirrors. τ and ψ: round-trip time and corresponding optical phase shift in the FP, respectively. τ_l and φ: round-trip time and phase shift between laser and FP, respectively. K: control gain comprising all losses on the round trip between laser and FP (including the factor $\sqrt{R}$ for a single reflection). K and φ are adjusted by a variable neutral density filter and a piezo positioning with high resolution (20 nm), respectively. Laser details: see text.

Multisektionslaser

(auch Stabilisierung des Exp. - cw möglich: Schikora et al, PRL (2006)) ohne Kontrolle

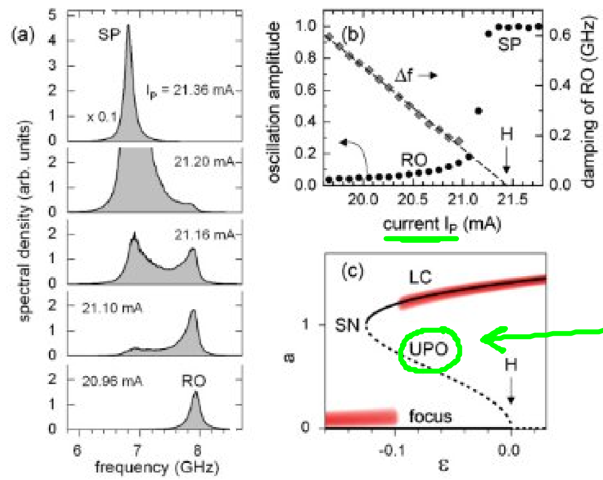

Ziel: Stabilisierung des UPO (Selbstpuls. mit kleiner Amplitude)

FIG. 2. (Color online) Subcritical Hopf bifurcation in the experimental device. (a) Power spectra of ROs and SPs for selected currents I_P. (b) Dots: amplitudes of ROs and SPs normalized to maximum versus I_P. Diamonds: damping of ROs; the linear extrapolation to zero defines the position of the Hopf bifurcation H. $(I_L, I_A) =$ (87.1,8.7) mA. (c) Corresponding scenario of a Duffing-van der Pol oscillator [31]. Lines: normalized amplitudes of deterministic oscillations and focus ($a = 0$) versus bifurcation parameter ε. UPO: unstable periodic orbit. SN: saddle-node bifurcation of orbits. LC: stable limit cycle. Gray (red) scale coded: normalized amplitude probability distribution (3) for noise level $D = 10^{-3}$. Probabilities below 1% are not shown.

$\lambda \hat{=}$

[31] Zakharova et al., PRE 81, 011106 (2010)

PHYSICAL REVIEW E **83**, 026203 (2011)

mit Kontrolle

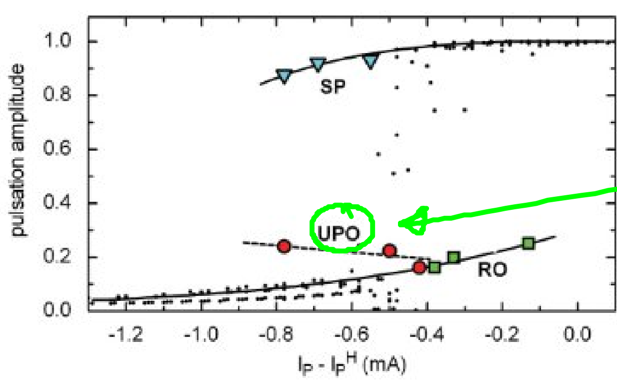

Stabilisierung des Odd-number orbits

$\hat{=} \lambda$

FIG. 3. (Color online) Control experiments at subcritical Hopf bifurcation: normalized SP amplitude versus distance to bifurcation. Cyan triangles: SPs stabilized with $\tau = 145$ ps, Green squares: CW emission stabilized with $\tau = 59$ ps. In both cases $R = 0.5$, $K = 0.02$. Red circles: UPO stabilized with $\tau = 130$ ps, $R = 0.3$, $K = 0.06$. The uncertainty of K is always about 15%. Black dots: Data of the free-running device, which are collecting measurements for all operation points used in the control demonstrations. Lines: guide to the eye.

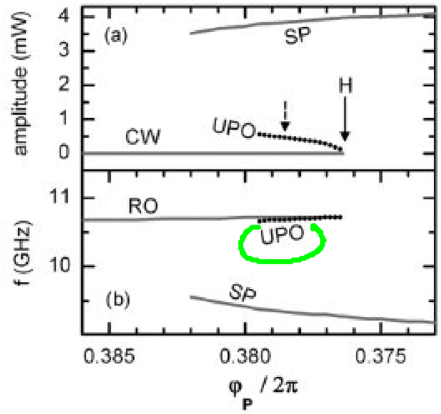

FIG. 5. Simulations of the control scenario. (a) Pulsation amplitude and (b) frequency versus internal phase shift in the AFL. Solid gray: stable states of the free-running laser [RO in (b): damped relaxation oscillations toward CW], black dotted: UPO stabilized with $\varphi/2\pi = 0.84$, $R = 0.3$, $K = 0.06$, $\tau_l = 0$.

Kontroll-Szenario:

geeignete Wahl des Phasenstroms der passiven Sektion

→ interne Phase φ_p

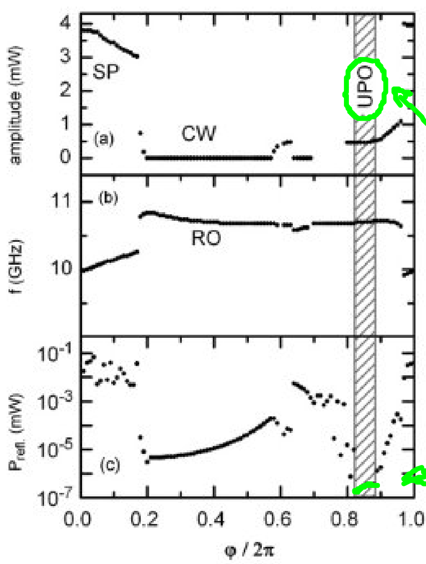

$\hat{=} \beta$

FIG. 6. Simulations of phase tuning. (a) Pulsation amplitude and (b) frequency versus control phase φ at $\varphi_P/2\pi = 0.3785$ for otherwise identical parameters as in Fig. 5. (c) Feedback power reinjected into the laser when stopping iterations. Shaded area: range for noninvasive control of UPO. Feedback power is here below 10^{-5} of laser output.

Stabilisierung nur möglich für endl. Kontrollphase

$\beta = \varphi$

nichtinvasive Kontrolle des Odd-number UPO

3.2.3 Chaos-Kontrolle durch zeitverzögerte Rückkopplung

Pyragas, Phys. Lett. A 170, 421 (1992)

$$\boxed{\dot{x} = f(x) + KA\left[x(t-\tau) - x(t)\right]} \quad x \in \mathbb{R}^n, \quad n \times n \text{ Kopplungsmatrix } A$$

$\dot{x} = f(x)$: chaot. Attraktor mit unendl. vielen UPOs

→ s. Kap. 2

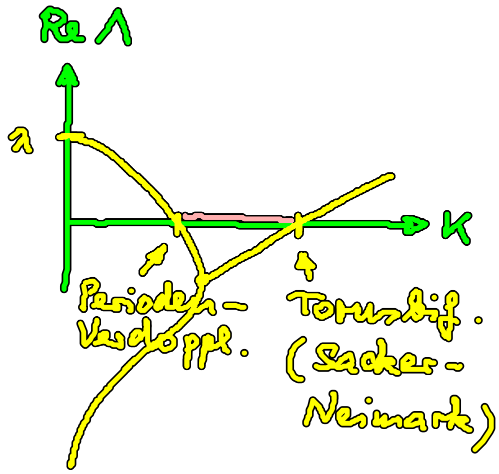

unkontroll. Floquet-Problem

$$\delta x = e^{\Lambda t}\, u(t), \qquad u(t) = u(t+T)$$

$$(\lambda + i\omega)\, u + \dot u = Df\, u$$

kontr. (diagonale Kontrolle)

$$\Lambda u + \dot u = Df\, u + \underline{K(e^{-\Lambda\tau} - 1)\, u}$$

Insb.

$$\Longrightarrow \boxed{\Lambda + K(1 - e^{-\Lambda\tau}) = \lambda + i\omega}$$

Schöll u. Schuster (eds.): Handbook of Chaos Control (2008)

3.2.4 Kontrolle raum-zeitlicher Systeme

Kyrychko, Blyuss, Hogan, Schöll: Chaos $\underline{19}$, 043126 (2009)

Gray-Scott-Modell (Reaktions-Diff.-System)

$U + 2V \to 3V$ $\qquad A \rightleftharpoons U$ $\qquad$ Aktivator u

$V \to P$ $\qquad\qquad\qquad\qquad$ Inhibitor v

$$\begin{pmatrix} \dot u \\ \dot v \end{pmatrix} = \begin{pmatrix} -uv^2 + a(1-u) + D_u \nabla^2 u \\ uv^2 - (a+b)v + D_v \nabla^2 v \end{pmatrix} + KA \begin{pmatrix} u(t-\tau) - u(t) \\ v(t-\tau) - v(t) \end{pmatrix}$$

bis zu 3 räumlich-homogene Fixpkte. $E_0 = (1,0)$ immer stabil

$E_{1,2}$ nichttrivial

Aktivator-Kontrolle $A = \begin{pmatrix} 1 & 0 \\ 0 & 0 \end{pmatrix}$

Inhibitor-Kontrolle $A = \begin{pmatrix} 0 & 0 \\ 0 & 1 \end{pmatrix}$